Small-Angle Light Scattering Calculations and Evaluation: Application to Phase Separation and Phase Dissolution Processes

Jaroslav Holoubek

Institute of Macromolecular Chemistry, Academy of Sciences of the Czech Republic, 162 06 Prague 6, Czech Republic

SUMMARY: The model calculations and corresponding experiments (time-resolved light scattering and image analysis) have been conducted to investigate the kinetics of phase separation and phase dissolution of polymer blends. The blends studied were polystyrene-d_8/polybutadiene (PSD/PB) and polystyrene/poly (methyl methacrylate) (PS/PMMA), both with or without diblock copolymers composed of the corresponding homopolymers, and a PS/poly(methyl vinyl ether) (PS/PMVE) blend. The time evolution of the spinodal peak position $q_m(t,T)$ and the scattered intensity maximum $I_m(t,T)$ at q_m have been compared with theoretically predicted values of exponents for distinct time scales of the phase dissolution in various temperature regimes.

Introduction

Various optical techniques have been investigated as potential candidates for characterization of multiphase polymeric materials. For design of new materials by polymer blending, one needs a basic understanding of phase behaviour-phase equilibrium, kinetics of phase separation and kinetics of phase dissolution in polymer systems[1]. Since the phase separation process is driven by the growth of fluctuations on length scales comparable with the concentration or composition fluctuations, which for polymers are typically of the order of 0.1 μm near the critical point, time-resolved light scattering (which probes the q range from 0.2 to 30 μm^{-1}, where q is the wavenumber of the fluctuations) has been widely used to examine phase separation kinetics in polymer blends[2,3] and solutions. Together with the time-resolved light scattering experiments the image analysis has been conducted to investigate the influence of diblock copolymers on the kinetics of phase changes of polymer blends. The values of the peak position $q_m(t,T)$ are related to the average or predominant phase-separated domain size d by $d = 2\pi/q_m$. The features of the spinodal peak position $q_m(t,T)$ and the

 CCC 1022-1360/00/$ 17.50+.50/0

maximum intensity $I_m(t,T)$ as a function of time, with and without copolymer additive, were analyzed for near- and off-critical composition in various temperature jumps. This type of experiment is usually termed the temperature jump light scattering experiment[3]. In kinetic studies, the variation of scattering intensity at various wavenumbers is studied as a function of time during a complete cycle consisting of a temperature drop from T_1 in the single-phase region to T_2 in the two-phase region (a period of spinodal decomposition), followed by a temperature change from T_2 back to T_1, and subsequent relaxation to the original equilibrium state (a period of phase dissolution).

Theoretical: Phase Separation and Phase Dissolution

Phase separation process

The time evolution of the spinodal peak position $q_m(t,T)$ and maximum scattered intensity $I_m(t,T)$ have been traditionally characterized by scaling laws with theoretically predicted values of exponents for distinct time scales of the phase separation process[4] (early, intermediate and late stages). It is very well known that in the early stage, the scaling theory predicts[4]

$$I(q_m) \sim \exp(2R_m t),\ q_m \sim t^o \qquad (1)$$

Similarly in the intermediate stage Eq. (2) holds

$$I(q_m) \sim t^{\alpha},\ q_m \sim t^{-\beta} \qquad (2)$$

and in the late stage then $\alpha = 3\beta$.

The intermediate and late-stage growth rates do not seem to follow a universal scaling function in the blend with the addition of diblock copolymers[3].

Phase dissolution process

The theory of dissolution predicts[5-7]

$$q_m(t,T) \cong t^{-1/2} \qquad (3)$$

and the peak intensity I_m should decrease exponentially as a function of time.

The time evolution of the spinodal peak position, $q_m(t,T)$, and intensity $I_m(t,T)$ have been compared with theoretically predicted values of exponents for distinct time scales of the phase dissolution in various temperature regimes.

Phase dissolution process and turbidity

In the early stage, the composition fluctuations are small and the light scattering theory based on the fluctuation concept can be used relating transmission properties to the size and amplitude of refractive index fluctuations. The expression for turbidity known from the Debye-Bueche theory can be used for calculations[8]. In the late stage the domains are growing in size becoming comparable with the wavelength of light used for illumination and the Lorenz-Mie (LM) description of light scattering processes is appropriate[8]. For scattering systems without any significant absorption, the diffuse approximation of the transport theory has been used.

Detailed numerical comparison showed that the results of the photon diffusion theory, Monte Carlo simulations[9] and of the Kubelka-Munk theory[10] are in very good agreement provided that the asymmetry factor[10,11] is incorporated into calculations of the extinction[12,13]. The use of the asymmetry factor reflects the fact that the classical assumption of independent scattering is not valid for a dense medium that contains particles occupying an appreciable fractional volume[10]. A reasonable agreement has been found between the experimental and calculated values of the scattering cross-section for various polymer systems up to a volume fraction of 0.2 under the diffuse approximation[13]. For this regime, the turbidity τ is given by

$$\tau = NC_{sc}(1-g) \qquad (4)$$

where N is the number of spherical particles per unit volume having radius r, C_{sc} is the scattering cross-section and parameter g is the asymmetry factor[8,10-13] (indicating an asymmetry of scattering intensity envelope by means of the average value of cos θ, where θ is the scattering angle).

The objective of the present chapter is to study the temporal evolution of turbidity and transmission in the model system of polystyrene/poly(methyl methacrylate) (PS/PMMA) blend at the late stage of the phase separation process (Oswald ripening), with the power law growth rate of domain sizes. The expression[12] for the transmittance T is

$$T = I/I_o = \exp(-\tau l) = \exp[-NC_{sc}(1-g)l] \qquad (5)$$

where I, I_o, τ, and l are the transmitted intensity, incident intensity, turbidity and path length, respectively. For the calculation of scattering cross-sections, asymmetry factors and corresponding turbidities, we used the Mie3 program[14] (implementation of the LM theory) and Eq. (4). We included in the calculations the effective refractive index of the medium in the form of a simple mixing rule[13].

Experimental and Materials

Optical and block scheme of the time-resolved small-angle light scattering set-up

The experimental set-up used for time-resolved light scattering measurements will be published elsewhere [15].

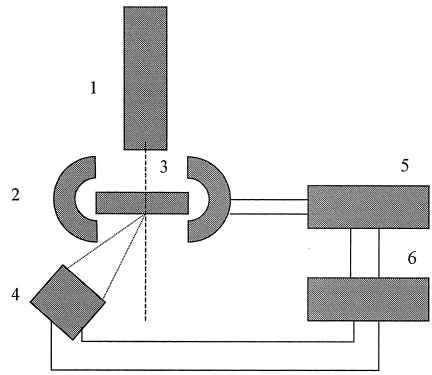

Fig. 1: Light scattering set-up for critical temperature determination: (1) He-Ne laser, (2) hot stage, (3) sample between silica glass windows, (4) photodiode detector, (5) thermal analysis system, (6) computer.

Figure 1 shows a simple light scattering apparatus[16] used for determination of binodal temperatures in studies of phase diagrams and kinetics of phase dissolution. The basic components are a He-Ne laser, a hot stage (Metler FP 800 thermal analysis system), a photodiode, and a computer with detection software. The hot stage can be programmed to provide isothermal setting and also linear temperature rise at different rates between 0.1 and 90 °C/min.

Materials

(1) PSD/PB blend[3]

polystyrene-d_8(PSD), $M_w = 1.0 \times 10^3$ g/mol, polybutadiene (PIB) $M_w = 5.3 \times 10^3$ g/mol, polystyrene-d_8-polybutadiene symmetric diblock copolymer(PSD-PIB), $M_w = 1.06 \times 10^4$ g/mol

(2) PS/PMVE blend[17], $M_w = 6.0 \times 10^4/6.4 \times 10^4$ g/mol

(3) PS/PMMA blend[18]

PS, $M_w = 8.9 \times 10^4$ g/mol, Polyscience; PMMA, $M_w = 7.4 \times 10^4$ g/mol, Pressure Chem., PS-*b*-PMMA copolymer 8.0×10^4 g/mol, Polyscience

Results and Discussion

Phase separation: PS/PMVE blend

The masks (motives) (Fig. 2a) based on micrographs of the PS/PMVE blend[17] have been used to study the breakup process of the co-continuous structure into discrete droplets. The corresponding diffraction patterns obtained by optical Fourier transformation are given in Fig. 2b. It can be seen that the diffraction pattern related to discrete droplets still shows high periodicity (diffraction "halo") and does not reveal the morphological change from the co-continuous structure into droplets. On the other hand, some statistical parameters obtainable from image analysis such as maximum of the intensity histogram (related to the probability density function of intensity p(I)) have extreme values as can be seen in Fig. 3. The value I_{max} is minimal for mask number 6, which corresponds to the point of morphology change.

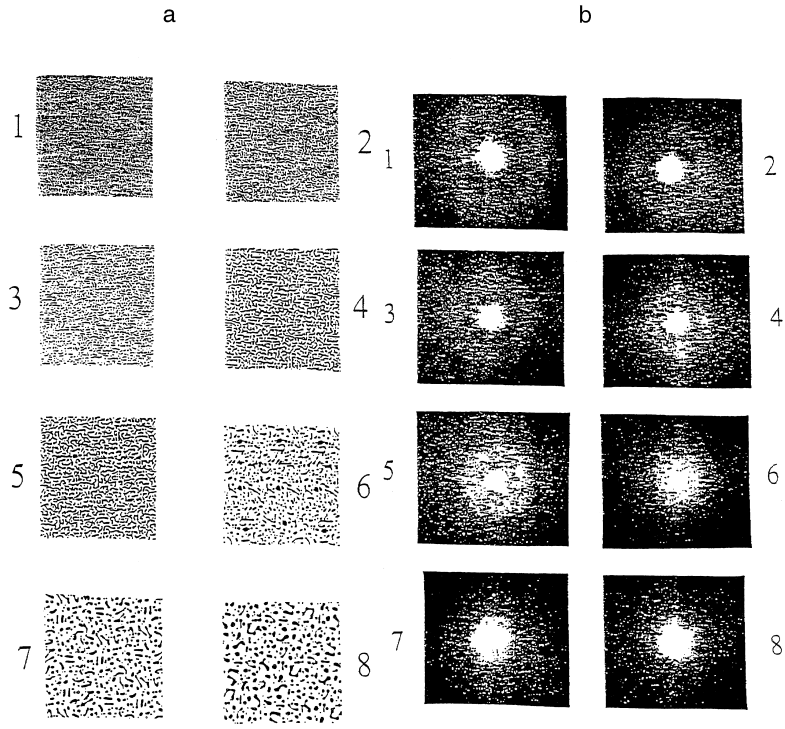

Fig. 2: Masks (motives) based on the micrographs of the PS/PMVE morphology in the late stages of spinodal decomposition, (b) corresponding diffraction patterns.

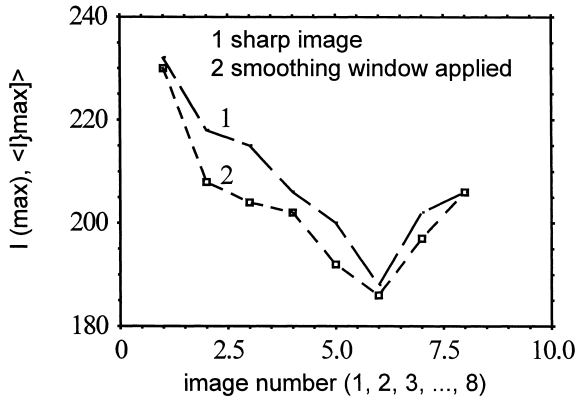

Fig. 3: Peak intensity of histograms corresponding to the masks from Fig. 2a.

It appears that the surface tension between the phases and redistribution of components are dominant factors in the dynamics of the morphological changes observed throughout the process and, even after the phase inversion point, we observe redistribution of components.

Phase separation: PS/PMMA model calculations

We follow the situation where the volume fraction of the minority PS-rich phase is less than the percolation threshold so that the domains of the PS-rich phase are dispersed in the matrix of the PMMA-rich phase. Lifshitz & Slyozov[19] and later on many others analyzed the growth of dispersed domains and found that the asymptotic growth law is of the form $R(t) \div t^{1/3}$. Huse[20] generalized the growth law by adding two multiplicative coefficients C_2 and C_3, which combine both the exponents in the form $R(t) \sim C_1 t^{1/3} + C_2 t^{1/4}$. Our calculations are based on the growth law in the form $R(t) \div t^n$, where the exponents n = 1, 1/2, 1/3 and 1/4 have been used[21,22]. We used the following refractive indices[23] at $\lambda = 0.6328$ μm: n(PS) = 1.58592 and n(PMMA) = 1.48679. The considered volume fractions of PS in PS/PMMA blend were 0.15 and 0.30. Two values of the starting domain size have been chosen, 0.01 and 0.1 μm. The calculations of extinction and turbidity proceeded as mentioned above. In Fig. 4, we can see the time evolution of turbidity for the PS15/PMMA85 blend with starting domain size 0.1 μm. The speed of the turbidity increase is proportional to the exponent of the time dependence in the relation domain size versus time.

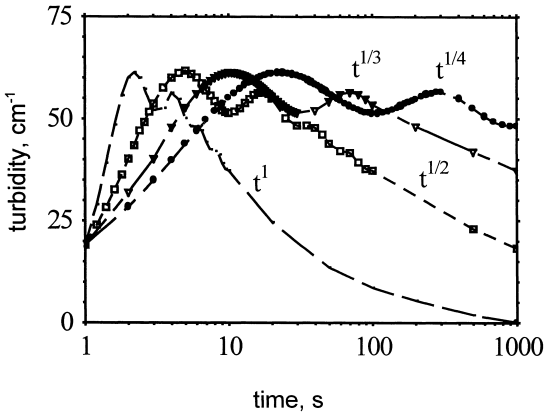

Fig. 4: Temporal evolution of turbidity for spherical domains of PS in PMMA. Volume fraction of PS=0.15. Starting domain diameter d = 0.1μm. The growth law is of the form $d \div t^n$, where n = 1,1/2,1/3 and 1/4.

Beyond the maximum value, the turbidity is decreasing in an oscillatory way: a small number of larger domains present at later stages of the phase separation show lower turbidity (keeping constant volume fraction of the minor phase). The calculation of time evolution of transmission for the same system with a smaller starting size of domain (0.01 μm) is shown in Fig. 5. It is worth mentioning that the range of "saturation" can be observed only for a sufficiently thin sample as of the presented thickness 100 μm. For thicker samples (l = 1 mm)

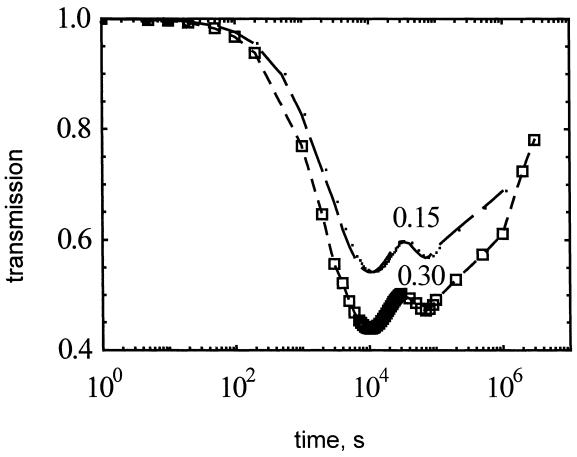

Fig. 5: Temporal evolution of transmission for spherical domains of PS in PMMA. Volume fraction of PS = 0.15. Starting domain diameter d = 0.01 μm. The growth law is of the form $d \div t^n$, the exponent n = 1/3 and 1/4. Sample thickness 1 mm and 100 μm.

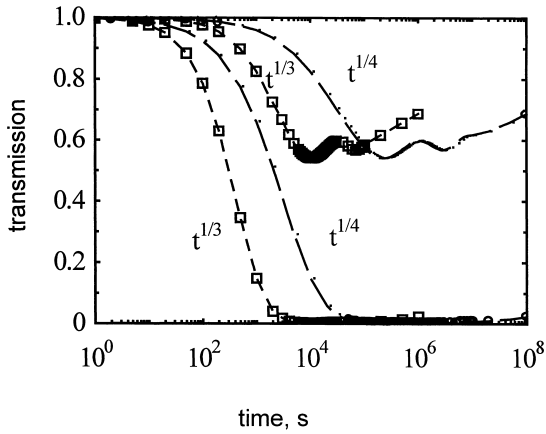

Fig. 6: Temporal evolution of transmission for spherical domains of PS in PMMA. Volume fractions of PS = 0.15 and 0.30. Starting domain diameter d = 0.01 μm. The growth law is of the form $d \div t^{1/3}$.

transmission decreases virtually to zero value and "saturation" cannot be observed. A comparison of time behaviour of transmission for systems with different amounts of the minor phase is given in Fig. 6. The light transmission is lower for larger volume fractions of the minor phase, as expected.

It can be concluded that

(a) Time evolution of turbidity and/or transmission reflects the temporal changes of the domain size very distinctly. (b) The absolute value of turbidity can be calculated from the known optical parameters of the separating components. (c) The "saturation" of transmission and eventual increase in transmission should be observed at later stages of the domain growth for thin (ca 100 μm and thinner) samples at constant values of volume fraction of the minor phase. (d) There exists an "induction" time for optical experiments where the temporal evolution of the size of separating phases has no observable effects on transmission (cf.[24]).

Phase dissolution: PSD/PB blend

We have expended effort to explain typical shapes of the obtained scattered intensity curves (cloud point curves) on the basis of the theory of dissolution and made a comparison with the experimental data obtained on a PSD/PB blend with various amounts of the PSD/PB diblock copolymer[16].

To compare theoretical and experimental data, we have chosen the following system parameters for calculations: blend PSD80/PB20 (w/w) in the temperature range 30-60 °C, the linear temperature rate 0.5 °C/min and angular integration range 10 degrees around the scattering angle 45° (Fig. 1). We anticipated a power-law behaviour of q_m in the form of Eq. (3) and an exponential decrease in the peak intensity as a function of time.

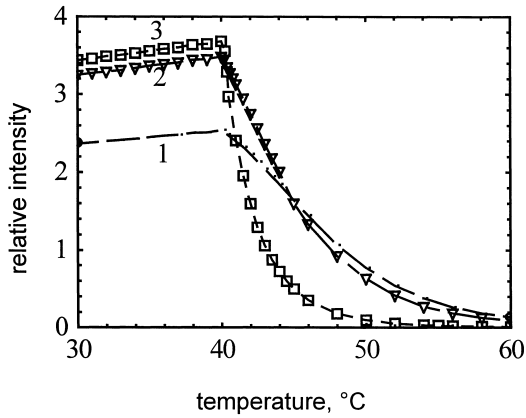

Fig. 7a: Theoretical temperature (time) evolution of scattering intensity for PSD80/PB20 blend. Linear temperature rate 0.5 °C/min. Co-continuous starting structure in two-phase region. Correlation lengths: (1) 0.3 μm, (2), 0.34 μm, (3) 0.445 μm.

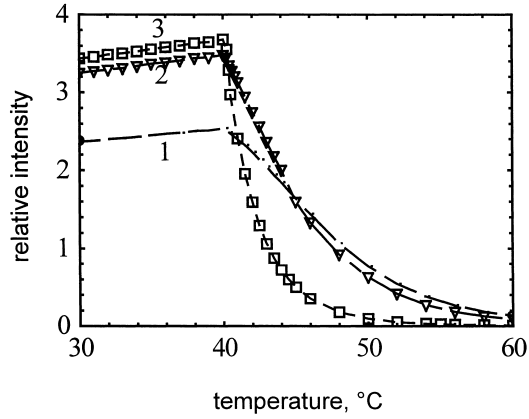

Fig. 7b: Theoretical temperature (time) evolution of scattering intensity for PS80/PB20 blend. Linear temperature rate 0.5 °C/min. Starting structure without an intensity maximum in scattering pattern. Correlation lengths: (1) 0.3 μm, (2) 0.34 μm, (3) 0.445 μm.

In Fig. 7a we can see the temperature and time evolution of relative scattering intensity for experimental set-up of Fig. 1 calculated for three correlation lengths when the starting samples have co-continuous structure. The critical temperature for all three samples is taken to be the same, i.e. 40 °C. An analogous calculation for the same starting sizes and equal critical temperature is in Fig. 7b for blend with starting morphology without an intensity maximum in scattering pattern. A comparison of theoretical (Fig. 7a,b) and experimental results[25] (Fig. 7c) confirms that the dissolution process can be reasonably modelled for this system using the above mentioned assumptions.

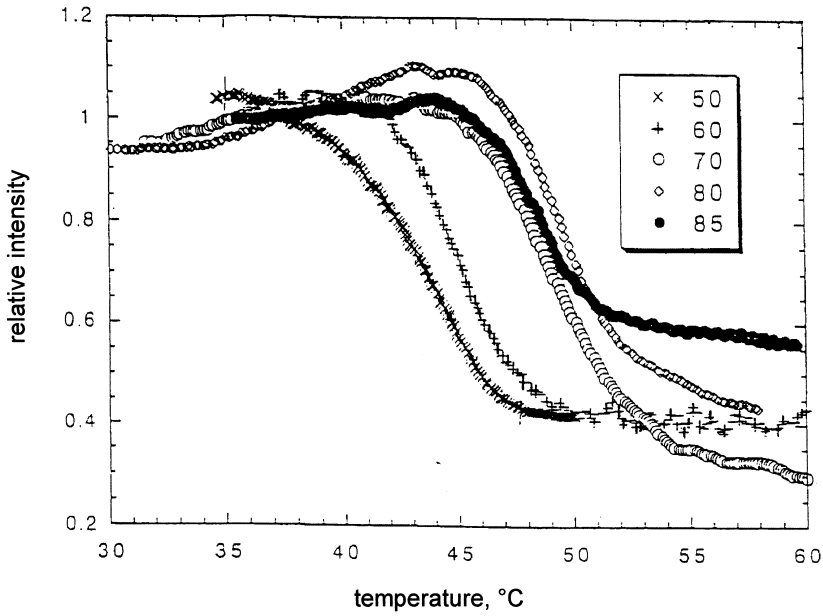

Fig. 7c: Experimental temperature (time) evolution of scattering intensity for various PSD/PB blends in the phase dissolution process (cf. set-up in Fig. 1), Linear temperature rate 0.5 °C/min. Volume fractions of PSD 0.5-0.85.

Phase dissolution: PS/PMMA blends

The size scale of the morphology observed by comparing the corresponding q_m for samples with and without the copolymer (cf. Fig. 8 and Fig. 9) was found to decrease with added diblock copolymer. The relative intensity plots with values q_m and $I(q_m)$ for samples with the copolymer are illustrated in Fig. 8 for annealing temperatures T = 130, 160 and 180 °C. Thirty

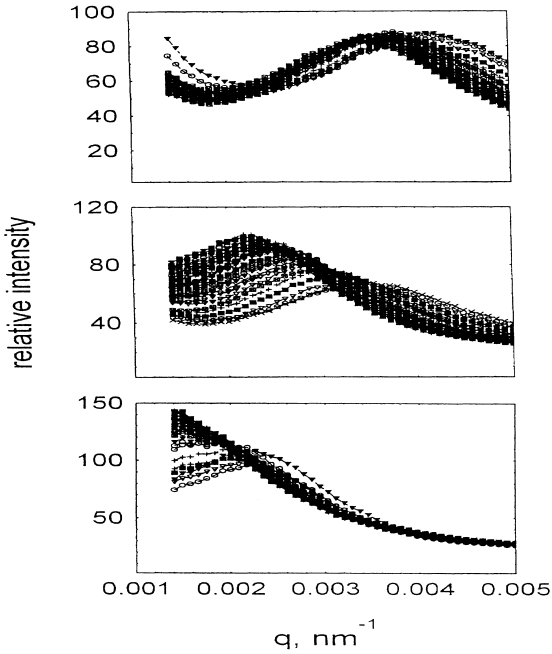

Fig. 8: Experimental time evolution of intensity profiles for the PS30/PMMA70 blend with 2 % of copolymer. 30 scans at given temperature with the time delay between scans $\Delta t = 90$ s. From the top: (a) T = 130 °C, (b) T =160 °C, (c) T = 180 °C. Shifts of the scattering maxima I_m to smaller q (to the left) are evident.

time scans at $\Delta t = 90$ s are presented for each temperature. Even though the exact localization of the copolymer is difficult, the phase contrast microscopy and comparable intensities $I(q_m)$ for samples without and with the copolymer confirm the co-continuous starting morphology in the two-phase region with most of the copolymer at the interphase. The interplay between the thermodynamic driving force exerting to decrease concentration fluctuations during annealing and that leading to the slowing down of the interdiffusion process due to the relative proximity of the glass transition is most apparent. At T = 130 °C, where the system is below the spinodal temperature (T_{sp} approx. 155 °C), the prevailing change in morphology is associated with the growing size of domains. The time evolution of the $I(q_m)$ is not so significant. The kinetics of coarsening and dissolution processes are different. This is because the growth occurring during the phase-separation coarsening process is influenced by a competition for material between the evolving phases, while the growth during the

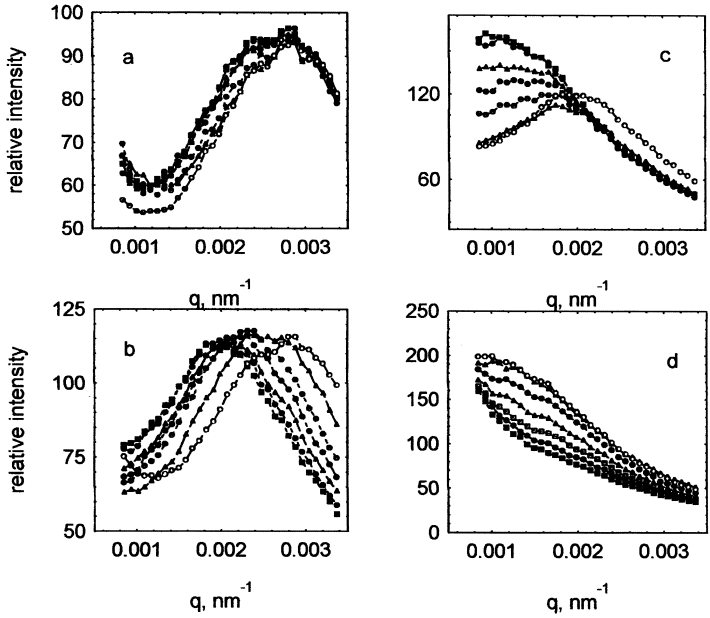

Fig. 9: Experimental time evolution of intensity profile for PS30/PMMA70 blend, annealing temperatures (a) T=130 °C, (b) T=160 °C, (c) T=180 °C, (d) T=200 °C. Selected curves with time delays between scans Δt= 9 minutes are illustrated. Starting curve (o), the last curve (□).

dissolution (annealing) involves the rate of bulk interdiffusion of the dissolving species. In our study, the dimensions of the phase-separated domains grow gradually during the annealing. The time evolution of q_m at T = 160 °C is presented in Fig. 10. The q_m values decrease almost exponentially with time rather than according to the power law (cf. Eq. (3)).

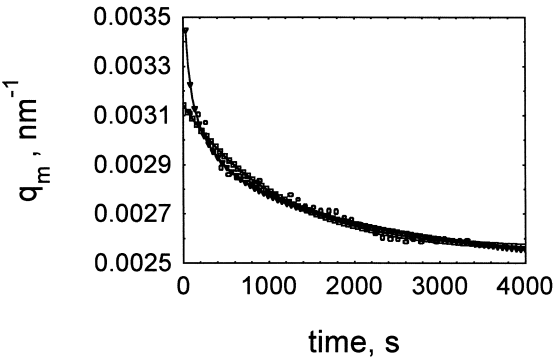

Fig. 10. Time evolution of q_m for the PS30/PMMA70 blend with 2 % of copolymer, T = 160 °C (see Fig. 6b). The exponential (□) and power law (▽) fits are illustrated.

Especially for higher annealing temperatures is the exponential fit substantially better then the power law fit. The power law exponent obtained from the fit in Fig. 8b gives 0.06, almost by an order of magnitude different from the theoretically predicted value 0.5. This low value might be influenced by the proximity of the T_g temperatures of both homopolymers, but further tests of this hypothesis are necessary. The same results are obtained from the power law fit in Fig. 8c. The decrease in $I(q_m)$ with time has not been observed for T = 130 °C. For higher temperatures of annealing, deviations from the exponential decay are observed especially during the initial time period. Experimental results for blends without the copolymer are presented in Fig. 9. The blends without the copolymer show larger starting domain sizes in comparison with the blends with the copolymer (cf. Figs. 8a, 9 and 11a,b) and the theoretically predicted evolution of $I(q_m)$ with time is partly followed in the given temperature regime. The temperature and time dependences of domain growth are

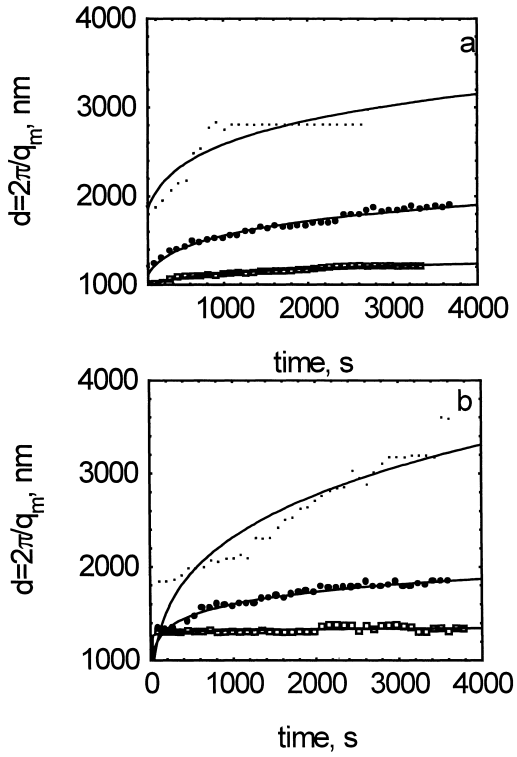

Fig. 11: Time evolution of domain sizes for (a) blend with 2% of copolymer, (b) blend without the copolymer. Annealing temperatures (□)T = 130, (•) T = 160, (o) T = 180 °C.

summarized in Fig. 11, for both types of polymer systems. The predicted power growth law based on Eq. (3) is indicated in the figures by full-line curves. For the lower annealing temperatures T = 130 and 160 °C, the shape of the size versus time curves corresponds to the power law type, but the exponents of the power law (ca 0.1) are much lower than the predicted value a=0.5. For the higher annealing temperature T = 180 °C, the power law dependence of growing size on time is evidently not fulfilled. The starting domain sizes are smaller for samples with addition of copolymer as expected (cf. Fig. 11a).

The theoretically predicted I_m intensity decay is confronted with experiment in Fig. 12a,b. It appears that the expected exponential decrease in I_m intensity is approximately appropriate for

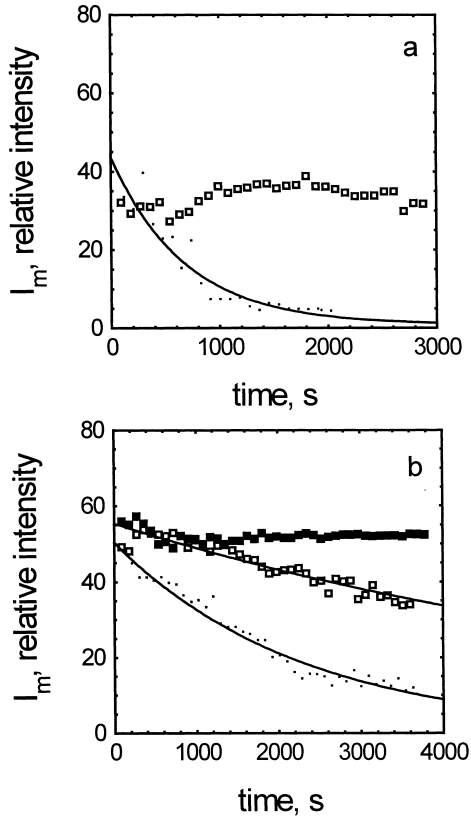

Fig. 12. Temporal changes of the intensity maximum, I_m, for the (a) blend with 2 % of copolymer, (b) blend without the copolymer. Temperatures (■) T = 130, (□) T = 160, (o) T=180 °C

describing the time behaviour of I_m of a simple homopolymer blend without the copolymer. It is interesting that the process of phase dissolution is slower for the system with the copolymer, where the change in I_m at the annealing temperature T = 160 °C is minimum. The I_m decay in time is postponed to a higher temperature, T = 180 °C. The effect of the copolymer on the slowing down of the phase separation process is very well known and the role of the copolymer in the " inversion" process could be similar.

Conclusions

(a) Image analysis of microscopic images at the phase inversion point indicates that the redistribution of components is an important factor in the dynamics of morphological changes.

(b) Time evolution of turbidity and/or transmission can be calculated from the known optical parameters of the separating components. The absolute value of turbidity, effect of "saturation" of transmission and "induction time" for optical experiments can be determined.

(c) Temperature evolution of the scattering intensity for PSD/PB blend in a simple scattering set-up can be modelled and reasonably corresponding to the experimental data.

(d) The dissolution process for the studied system cannot be reasonably modelled by a power-law decrease in the scattered vector q_m (in the form of Eq. (3) or equivalently by a power law increase in d_m values in time) and by an exponential decrease in $I(q_m)$ with growing dissolution time for the samples with the added copolymer in the ranges of temperatures used in experiment. Much lower exponents than 0.5 are determined from the dissolution experiments.

(e) The prevailing effect of phase dissolution for the PS/PMMA/PS-*b*-PMMA system in the studied temperature regimes is the growing size of separated domains. A non-exponential decrease in $I(q_m)$ is observed in the initial time period.

(f) The samples without the copolymer display larger starting domain sizes and the theoretically predicted $I(q_m)$ versus time behaviour is approximately followed in the given temperature regime.

Acknowledgements

We gratefully acknowledge support of the Grant Agency of the Czech Republic (Grant No. 203/99/0573) and of the Grant Agency of the Academy of Sciences of the Czech Republic (Grant No. A4050902).

References

1. J. D .Gunton, M. S. Migaud, P. S. Sahni, *Phase Transition and Critical Phenomena*, C. Domb and J. L. Lebowitz (Eds.), Academic Press, New York 1983
2. T. Sato, C. C. Han, *J. Chem. Phys.* **88,** 2057 (1988)
3. L. Sung and C. C. Han, *J. Polym. Sci:, Part B: Polym. Phys.* **33,** 2405 (1995)
4. T. Hashimoto, M.Takenaka, H. Jinnai, *J. Appl. Crystallogr.* **24,** 457 (1991)
5. A. Z. Akcasu, R. Klein, *Macromolecules* **26,** 1429 (1993)
6. A. Z. Akcasu, I. Bahar, B. Erman, Y. Feng, C. C. Han, *J. Chem. Phys.* **97,** 5782 (1992)
7. M. Best, H. Sillescu, *Polymer* **33**, 5249 (1992)
8. M. Kerker, *The Scattering of Light*, Academic Press, New York, 1969
9. L. Tsang, Ch. E. Mandt, K. H. Ding, *Opt. Lett.* **17**, 314 (1992)
10. G. H. Meeten, Ed., *Optical Properties of Polymers,* Elsevier, Appl. Sci. Publ., London 1986
11. H.C. van de Hulst, *Multiple Light Scattering: Tables, Formulas and Applications*, Vol.1 and 2, Academic Press, New York 1980
12. L. F. Gate, *J. Opt. Soc. Am.* **63**, 312 (1972)
13. J. Holoubek, *Opt. Eng.* **37**, 705 (1998)
14. G. Gouesbet, G. Grehan, B. Maheu, *Appl. Opt.* **22**,2038 (1983)
15. Č. Koňák, J. Holoubek, P. Štěpánek, in preparation
16. J. Holoubek, L. Sung and C. C. Han, *Eur. Symp. Polymer Blends*, Maastricht, 1996, p.46-48
17. S. Reich, *Phys. Lett.* A **114**, 90, 1724 (1986)
18. J. Holoubek, *Makromol. Chemie: Macromol. Symp.*(1999), in press
19. I. M. Lifshitz, V. V. Slyozov, *J. Phys. Chem. Solids* **19**, 35 (1961)
20. D. A. Huse, *Phys. Rev.* B**34**, 7845 (1986)
21. L. N. Andradi, G. P. Hellmann, *Polymer* **34**, 925 (1993)
22. M. A. Kotnis, M. Muthukumar, *Macromolecules* **25**,1716 (1992)
23. J. Holoubek and C .C. Han, *Polym. Mater. Sci . Eng.* **71**, 368 (1994)
24. X. He, J.-M. Widmaier, G. C. Meyer, *Polym. Int.* **32**, 289 (1993)
25. L. Sung, unpublished results